
<p>© Article authors. This is an open access article distributed under the Creative Commons Attribution-NonCommercial-NoDerivs licens. (http://creativecommons.org/licenses/by-nc-nd/3.0/).</p>	<p>ISSN online 2545-2819 ISSN print 0800-6377</p>
<p>DOI: 10.2478/ncr-2021-0012</p>	<p>Received: Aug. 2, 2021 Revision received: Nov. 28, 2021 Accepted: Nov. 29, 2021</p>

Resonant Frequency Ultrasonic P-Waves for Evaluating Uniaxial Compressive Strength of the Stabilized Slag–Cement Sediments



Per Lindh, PhD ^{1,2}

¹Swedish Transport Administration, Gibraltargatan 7, Malmö, Sweden.

²Lund University, Division of Building Materials, Box 118, SE-221-00, Lund, Sweden.

Email: per.a.lindh@gmail.com



Polina Lemenkova, MSc ³

³ Université Libre de Bruxelles. École polytechnique de Bruxelles (Brussels Faculty of Engineering), Laboratory of Image Synthesis and Analysis. Campus de Solbosch, Av. Franklin Roosevelt 50, Brussels 1000, Belgium.

Email: polina.lemenkova@ulb.be

ABSTRACT

Marine sediments can be stabilized by ultra high-strength binders: cement, Cement Kiln Dust (CKD) and slag. The properties of the stabilized soil indicate potential to their reuse. This study investigated the performance of the unconfined compressive strength (UCS) in the marine sediments stabilized by binder (cement, CKD, slag), tested by ultrasonic P-waves. Materials include 194 specimens collected from the port of Gothenborg. The experiment was performed in Swedish Geotechnical Institute (SGI). The UCS of specimens stabilized by different ratio of binders (cement, CKD, slag) was tested by resonance frequencies of the elastic P-waves. The significant increase in the UCS (>1500 kPa) was recorded for the highest values of CKD and cement, and low values of slag. The correlation profiles of low water/high binder (L_w/H_B) cement/slag (40/60%) were controlled by curing time. The slag–cement–CKD simplex tests demonstrated UCS of samples with low/high water content and various binder ratio of cement (kg/m^3). The ratio of cement binder and curing time play a critical role in the increase of UCS followed by mechanical properties of specimens and intensity of stress. The highest values exceed

1000 m/s in P-waves. The results shown high accuracy (97%) and non-contacting approach for testing UCS of sediments. Seismic methods can be applied to test the UCS of the stabilized sediments, and also *in-situ* via seismic CPT, surface testing or cross hole seismic testing.

Key words: civil engineering, geophysics, seismicity, cement, slag, geotechnical engineering

1. INTRODUCTION

Sustainable constructions require accurate evaluation of the suitability and strength of soils. This specifically concerns marine sediments stabilized by cement, cement kiln dust (CKD) and slag for evaluating their properties prior to further re-use. Because the existing techniques do not fully satisfy to the geotechnical needs for non-destructive methods, there is a demand for development of the advanced methodologies for testing compressive strength of the stabilized soils. This paper presents a workflow for evaluating compressive strength of the marine sediments using seismic testing applied to various ratio of water/binder in the tested samples.

Cement is the most widely used binder in the construction works [1]. Due to its physical-chemical characteristics, it is applicable in solid structures [2–3], which results that global cement production exceeded 4.91 B Tons in 2020 [4]. To avoid the expensive costs for repairs of the concrete structures, such as roads, buildings, tunnels and bridges [5–8], the durability of solid materials should be evaluated by testing the compressive strength [9–11] and validating its suitability [12–14]. To meet this need, many experimental studies have been undertaken to develop, evaluate and standardize tests on the materials properties for compaction and compressive strength [15–21]. Although traditional test approaches are widely used in industry, they mostly have destructive nature and impose damage in specimen structures [22].

Therefore, besides existing methods on the compressive strength, an improved method has been developed aimed to use seismic resonant frequency measurements. This method is based on measuring the acoustic resonance of waves in order to evaluate the vibration of specimens. Estimating P and S wave velocities on the demoulded specimens of concrete is presented in various studies [23–28]. Its physical principle consists in the increasing amplitude of waves when frequency of the applied force is close to the natural frequency of the materials [29]. When oscillating force is applied at resonant frequency with maximum response amplitude, a specimen oscillates at a higher amplitude that can be measured [30–31]. Therefore, resonant frequency of cement specimens can indicate their physical properties and compressive strength.

The geophysical properties of solid structures are largely controlled by their mechanical properties: fabric, stiffness, volume, permeability, porosity, mineralogy [32–33]. For example, there is a correlation between the elastic compressibility and conductivity of the saturated rocks with porosity [34], gas hydration [35–37], or hydrate saturation in the clay-rich marine sediments with compressional wave and shear wave velocity [38]. The geometrical properties of specimen (e.g. dimensions, curvature, angularity, roughness) may also play a role in compressibility of the materials. Combination of marine geologic sampling and geophysical seismic measurements enable to evaluate geotechnical performance of soils more precisely, accurately, and using non-

contacting methods. At the same time, the geophysical properties of the materials are well reflected in seismic resonance frequencies that can be used to measure their compressive strength.

Measuring the compressive strength of concrete was advanced early by the uniaxial or triaxial tests as a traditional testing method [39–43]. Many industrial cases present measuring the compressive strength by uniaxial testing. This method is widely used due to the speed and convenience of applications in masonry, constructing tunnels, roads and buildings [46–48]. However, its disadvantage compared to the seismic method is that it is too sensitive to minor local variations in the specimen and very specific to the microstructure of cement, while seismic tests enable more general observations and can be applied to detect microcracks in the brittle solids [44]. For instance, using piezoelectric transducers enables to detect micro processes in solid samples by seismic measurements. Seismic velocity in the P- and S-waves changes in brittle rock: during hydrostatic loading, cracks close and velocities increase, during loading, new cracks form and velocities decrease in directions perpendicular to cracks [45].

Another example of the advantages of seismic treatment compared to the existing approaches, consist in the non-destructive nature which enables repeatability, without affecting the properties of the specimen. In contrast to the uniaxial tests, the growing body of the ultrasonic wave measurements [49–52] indicate that seismic testing is a more advanced method which uses remote sensing approach rather than direct contact with soil specimens. Correlation between the thickness of the added cement mortar and dynamic behaviour of the rock masses can be measured by seismic wave propagation [53].

A wider pool of published reports innovative applications of the remote sensing methods in civil engineering demonstrating general trends and specific nuances of seismic waves behaviour in cement mortar and concrete [54–58]. For instance, using computer vision for assessment of colour of stones/specimen based on their spectral reflectance and cross-section techniques [59–60], statistical analysis and scripting [61–62]. Such methods have a high potential but the prevalence of the traditional methods in measuring compressive strength is still far higher. This may be due to the fact that seismic testing methods in concrete studies require special software for data analysis, and availability of the devices in the laboratory.

Geophysical variability of binder properties regarding the proportions of added slag/cement and dependance on time of the experiment have led us to hypothesize that seismic P-waves velocity varies depending on binder content. Thus, using ultrasonic waves for resonant frequency seismic measurements is a valuable and effective yet underutilized tool for testing compressive strength of the stabilized soils. The present study considers implications of a mixture in percentage of cement in specimen (40/60% or 50/50% cement/slag combination) for assessing their compressibility measured by P-waves velocity changed over time (7, 14, 21 and 28 days). This well contributes to the existing studies showing changed properties of cement mortar with additions, e.g. alkali-activated slag, alkaline resistant glass fabric, ash in various proportions or reinforced concrete [63–68].

Accurate evaluation of the compressive strength of stabilized soils by seismic methods is a modern approach. It can effectively be applied to a highway engineering and construction of tunnels, bridges and highways [69–72]. The presented modelling and data analysis reports have shown

that test time and cement content in a binder are critical for measuring compressive strength by seismic waves velocity, while composition of the dredged masses (i.e. organic content) is a secondary factor that also affects the curing process. Modelling correlation between the porosity and seismic velocity in solids is a fundamental goal of numerous civil engineering studies [73–75]. Resonant frequency testing of the compressive strength, compared to the traditional methods in civil engineering [76–77] is non-destructive and environmentally sustainable approach. Seismic measurements are based on the remote sensing principles using geophysical properties of materials [66–69, 78–81].

2. MATERIALS AND METHODS

The objectives of this study was to apply precise, accurate and non-destructive testing by seismic sounding to characterize the compressive strength properties of sediment samples with varying proportions of cement using a wide frequency of P-waves at 7, 14, 21 and 28 days. The effects of applied strain, different geometries and dimensions of specimens and analysis of suitability of the specimen are studied in this research. The methodology is based on the existing standards of seismic measurements of sub-surfaces in geotechnical and civil engineering according to the Swedish Standards [82–83].



Figure 1. Photo showing specimens (sediments stabilized by cement in various proportions) cast in sampling sleeves stored in the water bath. Photo by Per Lindh.

2.1 Experiments

The dredged specimens of the marine sediments (Figure 1) were collected in the port of Gothenburg. All specimens were managed using the identical methodology. The laboratory

experiments have been performed within the framework of the Arendal 2 project in the SGI laboratory in Linköping, Sweden. The moisture state during measurements corresponded to the seawater proportion used in the tests with varied ratio of slag/cement (40/60% to 50/50%).

During the pre-processing we prepared two different mixtures of specimens in plastic barrels with various proportions of binder and water. The samples were mixed in barrels during five minutes using mortar and standard equipment following existing standards. The homogenization aimed to obtain a mixture and prepare stabilized samples in different ratios of water/binder. Afterwards, the specimens were stored in sampling sleeves stored in the water bath (Figure 1).

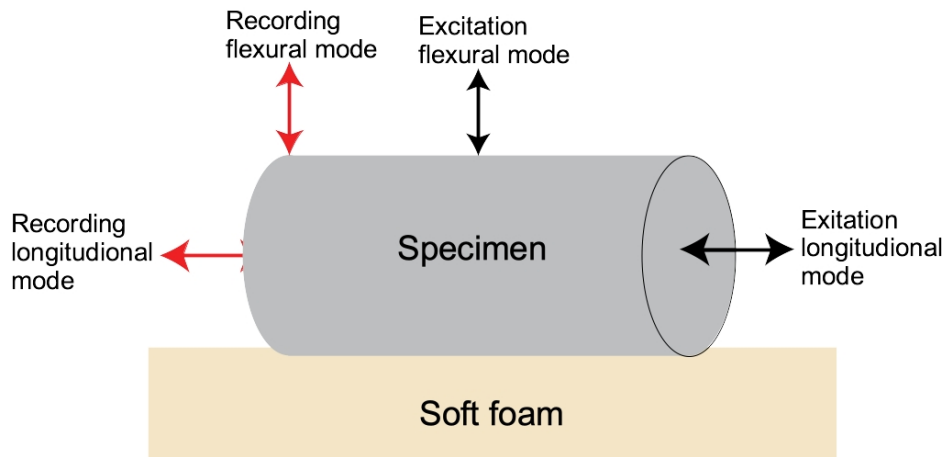


Figure 2. Schematic arrangement of the resonant frequency measurement of P- and S-waves.

2.2 Determination of P and S wave velocities

The theoretical background of the methods of measuring properties of the cement paste is based on the fundamental properties of solids that can be either elastic or inelastic depending on their reaction to the external stress pressure: compression, tension, shearing [84]. The P and S wave velocities were determined on the demolded specimens using measurements of the resonance frequency of P-waves (Figure 2). This approach measures the velocities of seismic waves (P and S waves) that pass through the solid material and differ according to their properties [85].

Both P-and S-waves belong to the seismic body waves that travel through solid in the directions controlled by their geophysical properties: density and modulus (stiffness), temperature and mechanical composition. The P-waves are compressional longitudinal waves, while the S-waves are shear transverse waves. This is well reflected in the existing definitions: “P-wave is an elastic body wave or sound wave in which particles oscillate in the direction the wave propagates” [86]; “S-wave is an elastic body wave in which particles oscillate perpendicular to the direction in which it propagates” [87]. In this study we used P-waves.

2.3 Measuring resonant frequency

The measured value of the resonant frequency of the sediments well indicated the compressive strength of specimens. The advantage of this type of measurement is that it is a non-destructive approach that can be repeated a large number of times without affecting the properties of the specimens. The increase of strength was monitored by the repeated measurements on the same specimen at a different curing time. The reference testing was performed using given samples.

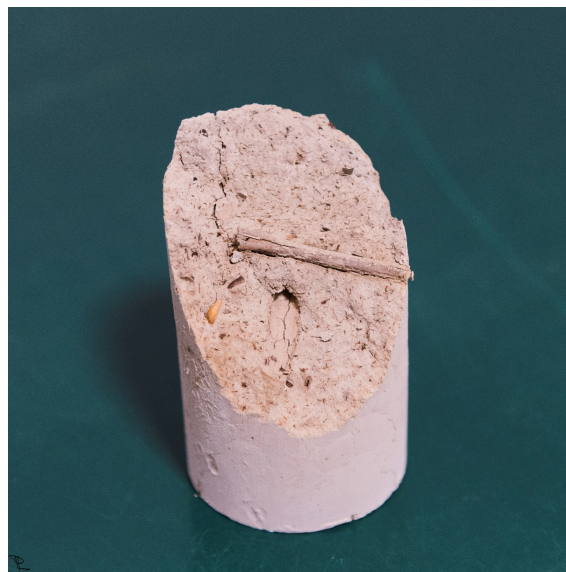


Figure 3. Photo showing fracture surface of the stabilized specimen. Note the reed piece directly exposed in the fracture plane. Photo by Per Lindh.

2.4 Seismic testing

The advantages of seismic testing compared to the uniaxial testing is that seismic test is a novel non-destructive approach used to characterize cement binders in various combinations of the proportions (cement/slag/water ratio). Thus, the testing is based on measuring resonant frequency of specimens to analyse the properties of the sediments. Another advantage is that this method is not sensitive to minor and micro local variations in the specimen itself (Figure 3). The position and orientation of the specimens (Figure 3) slightly affected the compressive strength.

It should also be noted here that the compressive strength is used to evaluate whether the binder specimen and its amount are sufficiently representative for the structure of specimen. In a large volume, the external inclusions do not play any role in terms of the entire volume control, but can still influence the choice of binder.

2.5 Workflow

To study aimed to evaluate the influences of the water/binder ratio in various proportions of binder (cement, CKD, slag), curing time, sample variety, and intensity of compression on the properties

of the stabilized marine sediments collected from the Gothenborg port. To achieve this aim, we measured sediment specimens in SGI using the defined workflow. The workflow followed the existing methodology [89] and existing Swedish Standards for geotechnical works.

The resonance frequencies of specimens with varying percentage of cement/slag/water content have been tested by measuring the vibrations generated by the P-waves. The resonant seismic excitation was performed by the effect giving vibration of specimens over the frequency range and measured at various curing periods (7, 14, 21 and 28 days).

The contaminated sediments were dredged from the coastal areas, solidified and stabilized (S/S) against erosion [90]. The specimens were stabilized by various combinations of cement, cement kiln dust (CKD) and slag. This enabled to test how the compressive strength of soil increases. Testing strength of the stabilized soil is necessary to assess its suitability for possible reuse in the constructions of roads, tunnels, highways and buildings. Thus, the aim of the physical testing on stabilization is to analyse if the stabilized sediments are suitable for reuse.

The statistical data analysis included plotting ternary diagrams by available techniques [91]. Ternary plots correspond to the trilinear coordinates showing the dependencies and correlations between the variables [92]. In this case, variables correspond to the proportions of binders: cement, slag and cement kiln dust (CKD).

3. RESULTS

The robust results evaluating optimal ratio of binder are obtained from the series of seismic and compressive strength tests. This also demonstrated the benefits of the double sampling.

Figure 4 shows variations in the P-waves velocities recorded in the reference samples that are monitored on day 7, 14, 21 and 28, respectively. Three important factors in evaluating the compressive strength included the following parameters: 1) the proportions of cement/slag; 2) the magnitude of stress (the intensity of compression); 3) the period of distortion for the cement specimen (strain rate estimated for 7, 14, 21 and 28 days of curing).

The grey dots in Figure 4 are taken from the pilot experiment at Arendal where the mixture has been performed *in situ* but the samples were stored in a laboratory under the same environmental and air conditions as the samples in this study. The result of mixture with 40% cement and 60% slag well corresponds to the result of the pilot Arendal experiment with 50% cement and 50% slag. The unconfined compressive strength (UCS) was determined according to the ISO/TS 17892-7 [88]. The figure shows that there is a good correlation between the P-wave velocity, compressive strength and curing time for the same water/binder ratio and binder content.

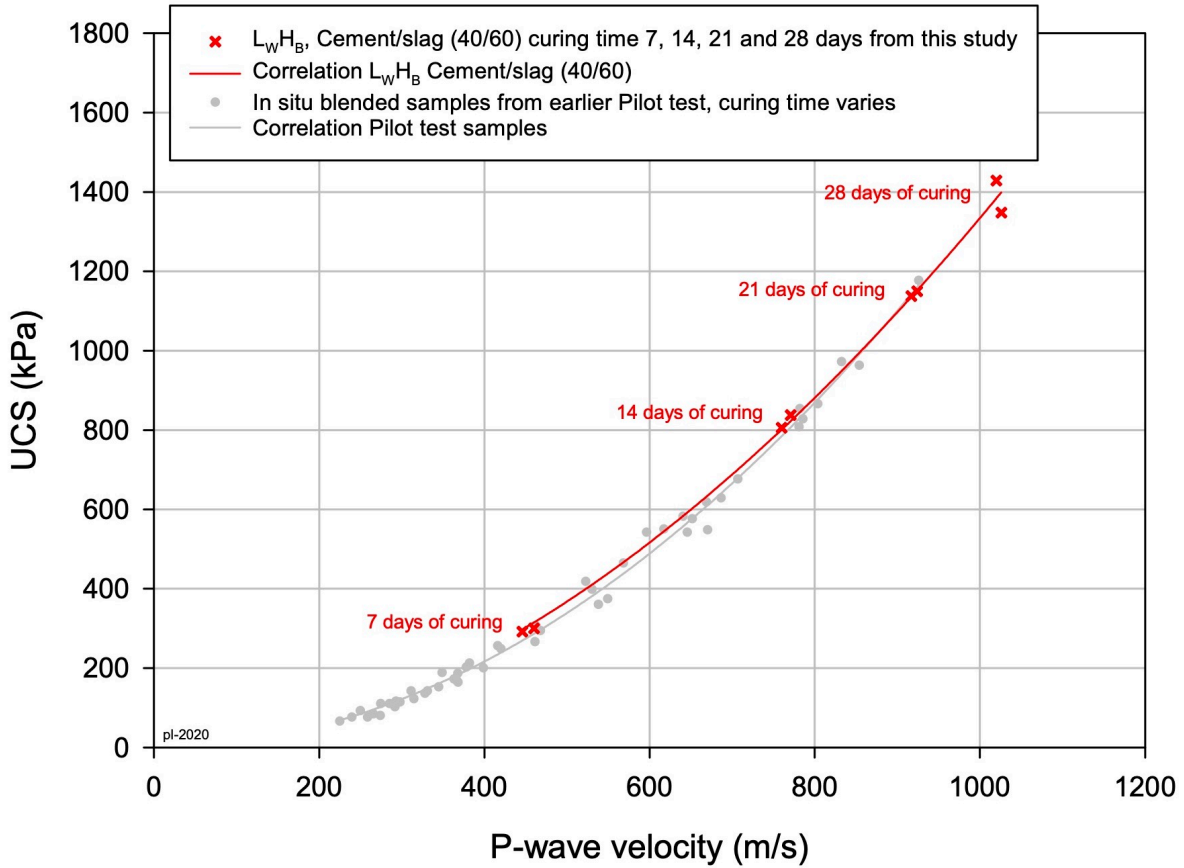


Figure 4. Graph showing correlation between variables: UCS (kPa) P-wave velocity and compressive strength of the stabilized sediments low water content/high binder (L_w/H_B).

The samples were processed during 91 days and then clustered into three major groups of binder (cement, CKD and slag) with variations in percentage as shown on the ternary diagrams (simplex plots). Within various sediment samples (Figure 4), tracking changes in P-waves frequency across specimen (cement/slag/water in percentage proportions) revealed geophysical dynamics and variations in the compressive strength that changed over time lasting from one week up to three months, i.e. 7, 14, 21 28 and 91 days (Figure 5). In the project, some extra samples were made specially to follow the dynamical growth of the compressive strength over time. These samples were tested after 7, 14, 21, 28 and 91 days.

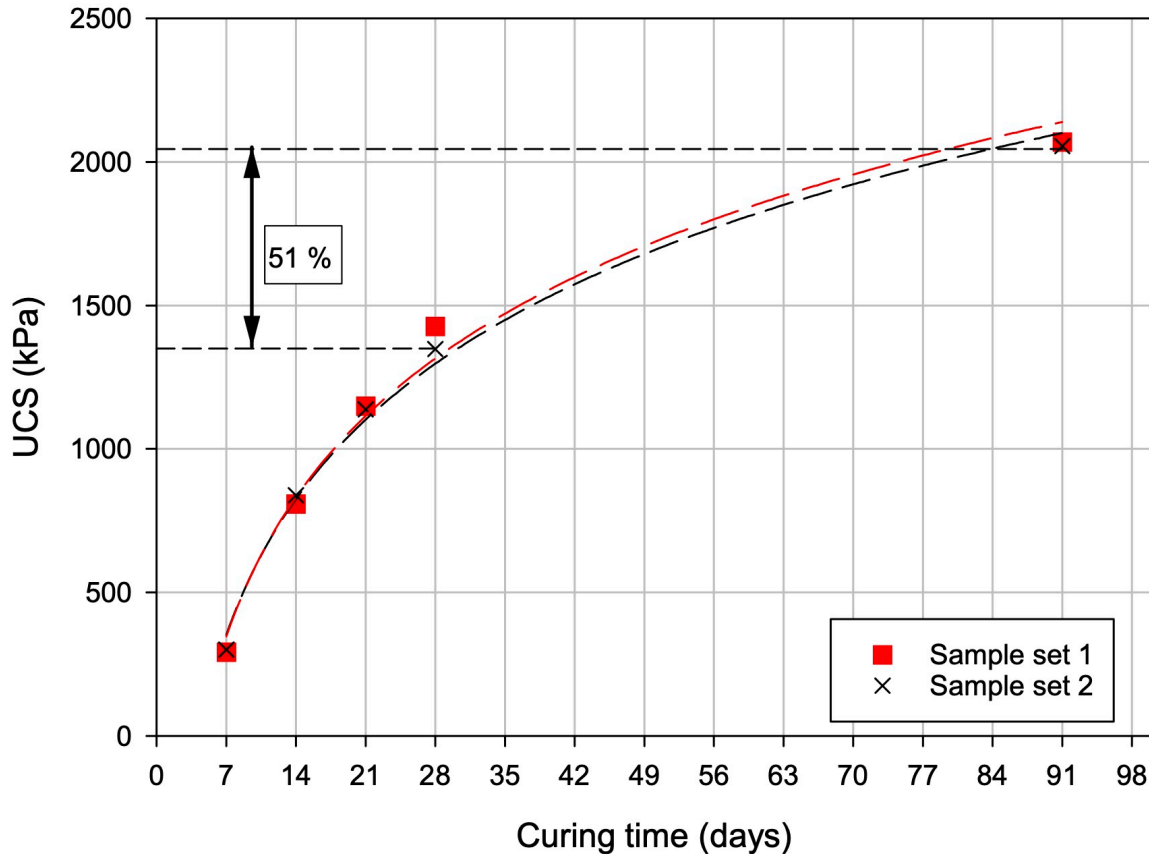


Figure 5. Functional correlation of the compressive strength with storage time. The figure shows a 51% growth of the compressive strength between 28 and 91 days.

3.1 Geotechnical parameters: temporal variability

Normally, the final strength is one of the most important parameters. However, in this project, we needed to get a more detailed evaluation of how the strength changes over time. Therefore, extra specimens were made for the evaluation of strength on days 7, 14, 21, 28 and 91 (Figure 4). The overall increase in the compression with P-waves velocity is visible in Figure 4. The highest values overstep 1,000 m/s in P-waves which corresponds to the 28 days of curing.

The correlation profiles of the L_W/H_B cement/slag (40/60) were clearly controlled by the time of curing (linearly increasing by the 2–5 month), and demonstrated a notable correlation with the *in-situ* blended samples taken from the previous experimental tests (Figure 4). However, this procedure required 10 specimens to be specially manufactured for each experimental set, which is both time-consuming and costly in terms of the study feasibility. Instead, a much simpler and faster procedure was applied using seismic resonant frequency measurements.

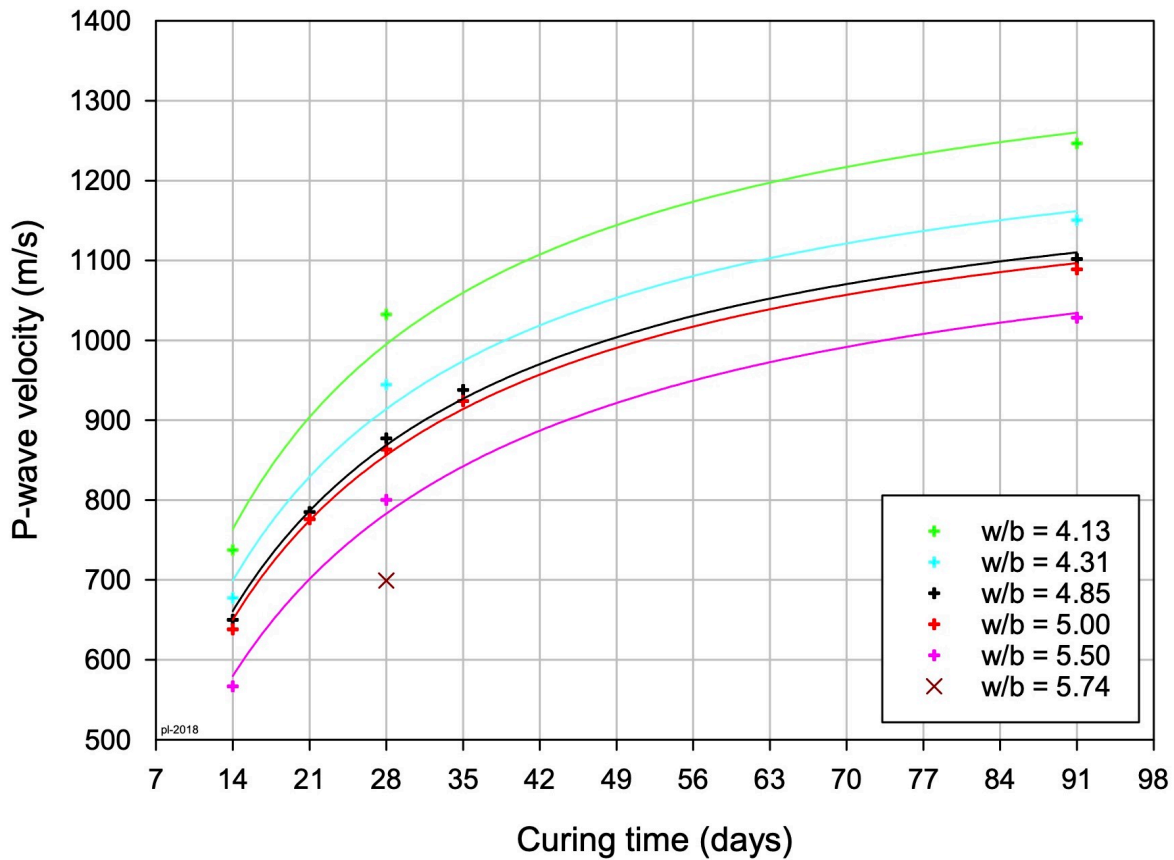


Figure 6. Graph showing the P-wave velocity as a function of storage time for the same sediment with the six different water/binder ratios.

3.2 Resonant frequency measurements: variations of P-wave velocity

Using resonant frequency measurements, the same sediment specimens have been measured repeatedly for water/binder ratio, without affecting the final results (Figure 6 and Figure 7). The regression lines (Figure 6) are based on the average of the four samples at each measuring point. The binder consisted of 40% cement and 60% slag. For $w/b=5.74$, we only measured values that are available for the 28th day of storage.

The regression lines have a hyperbolic shape (a more detailed report for the Nonlinear Regression from the Sigmaplot is presented in the Appendix A). The results demonstrated in Figure 6 show the expected model, i.e. low water binder numbers in general give higher P-wave velocity, which indicates higher compressive strength. The proportions of binder used in this case were as follows: 40% cement and 60% slag. When using pure cement (without addition of slag), a different result was obtained (Figure 7).

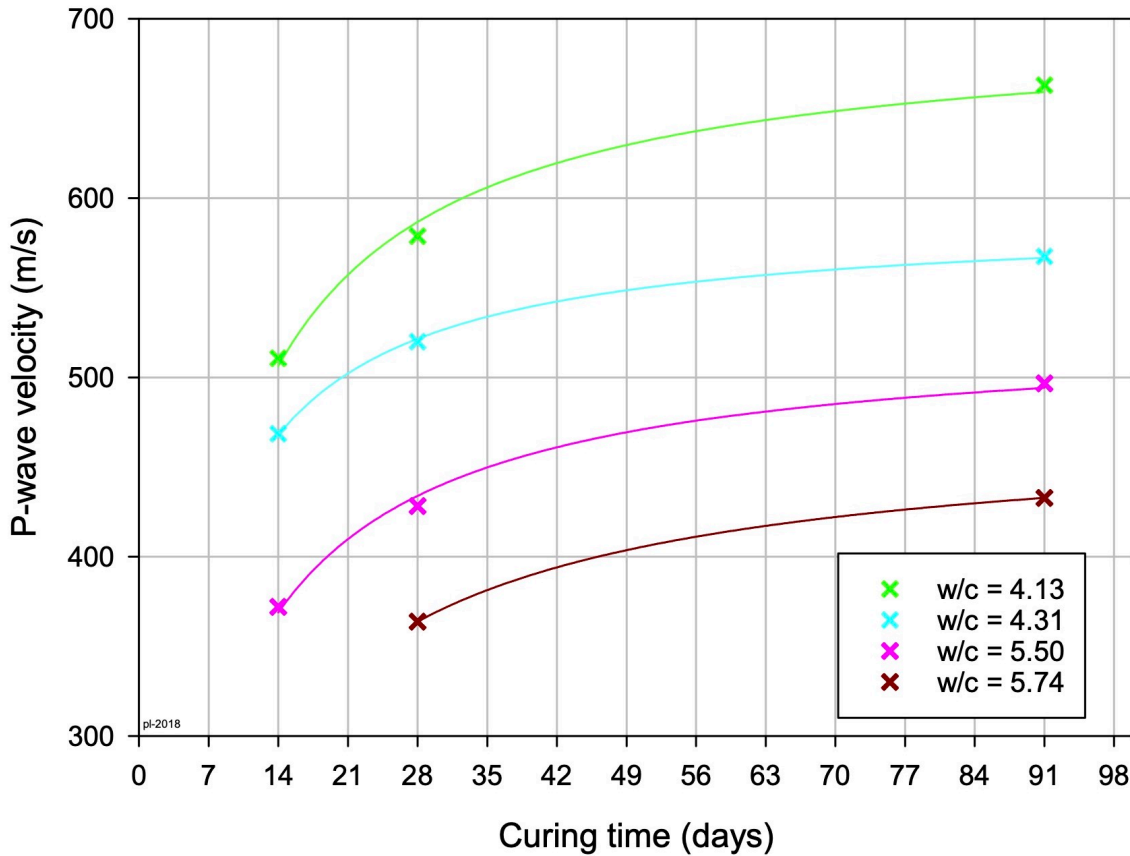


Figure 7. Graph showing the P-wave velocity at different storage times for different water cement ratio (W/C ratio).

As shown in Figure 7, for $w/c=5.74$, measurements were only available at 28 and 91 days, because the specimens were too soft to handle at the 14 days. In this case the regression lines are based on an average of four samples at each measurement point. In the processing of specimens, only CEM I was used as a binder. The individual variations in the strength of specimens were measured using values of resonant frequency of the P-waves (Figures 6 and 7).

These measurements also show the expected results on the compressive strength estimation. However, it should be noted that the difference in the results between the graphs shows that the relationships are unique for each binder combination. In this case, the main reason for the difference is because different binder compositions react with varying velocity in the curing process. The second reason is that the composition of the dredged masses (organic content in the sediment samples) also affects curing process during the experiment.

The advantage of the non-destructive testing is that even samples that are specially prepared for chemical environmental analysis can still be used without affecting and biasing the result. This means that more samples can be obtained. This makes the experiment statistically more sound and valuable. The accuracy of measurements of the seismic tests is higher and demonstrate less sensitivity to the initial set-up of the experiment compared to the traditional approaches.

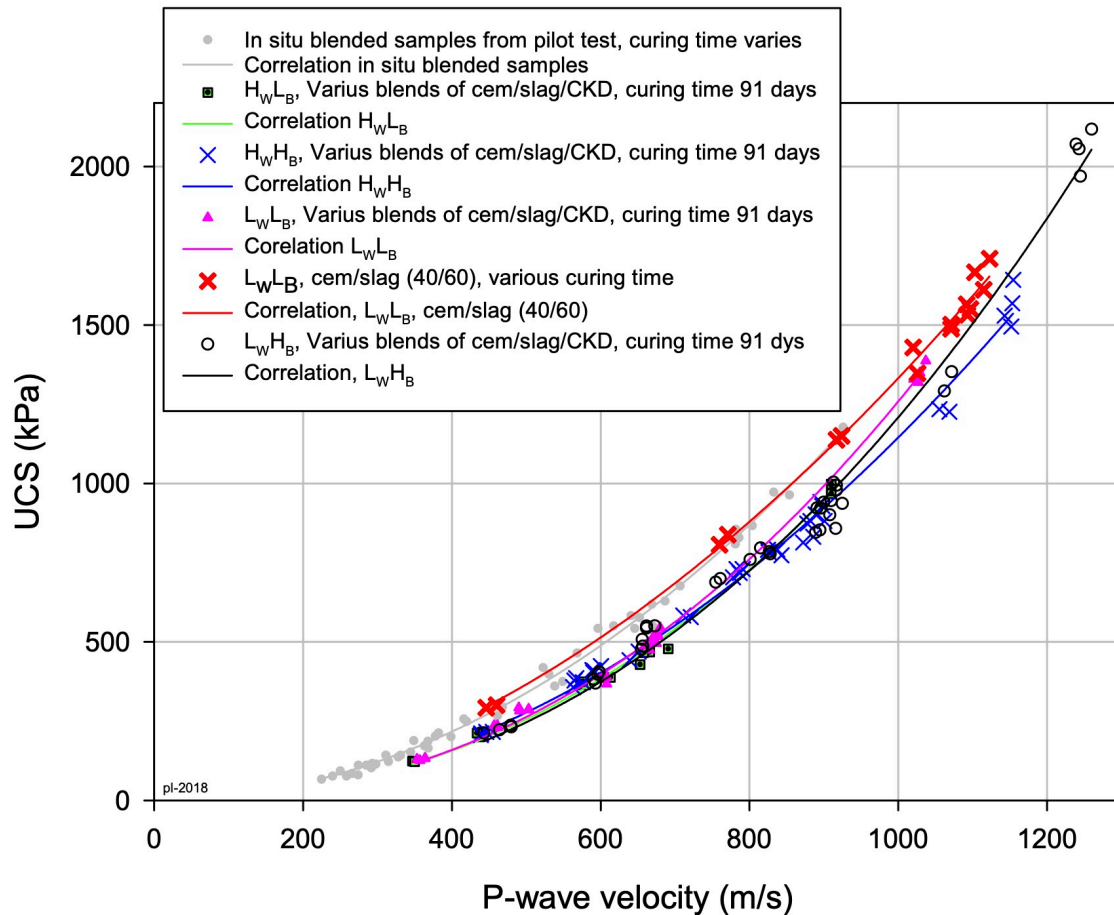


Figure 8. Correlation between the P-wave velocity and compressive strength of the stabilized sediments. The graph also reports the results from the samples taken during the pilot experiment. The abbreviations have the following meaning: High water content in combination with low binder = H_w/L_b ; High water content in combination with high binder = H_w/H_b ; Low water content in combination with low binder = L_w/L_b ; Low water content in combination with high binder = L_w/H_b

3.3 Correlation between the P-wave velocity and compressive strength

The correlation between the P-wave velocity and the compressive strength has been modelled and visualized in Figure 8. Here the abbreviation H_w/L_b stands for high water content in combination with low binder, while L_w/L_b stands for low water content in combination with low binder, and soon with the similar logic (see detailed capture in Figure 8). It shows the results of the P-wave measurement, before determining the uniaxial compressive strength of the specimen. This relationship has been used to compare different combinations of binder and used in checking reference samples from the *in situ* testing. Figure 8 shows samples included both in the current

and in the pilot experiments. Different samples were collected in current experiments: H_W/L_B (green dots), H_W/H_B (blue crosses), L_W/L_B (purple triangles) and L_W/H_B (transparent black circles), so the individual samples were highlighted for the statistical clearance of the experience. The result of Figure 8 can also be compared with Figure 4.

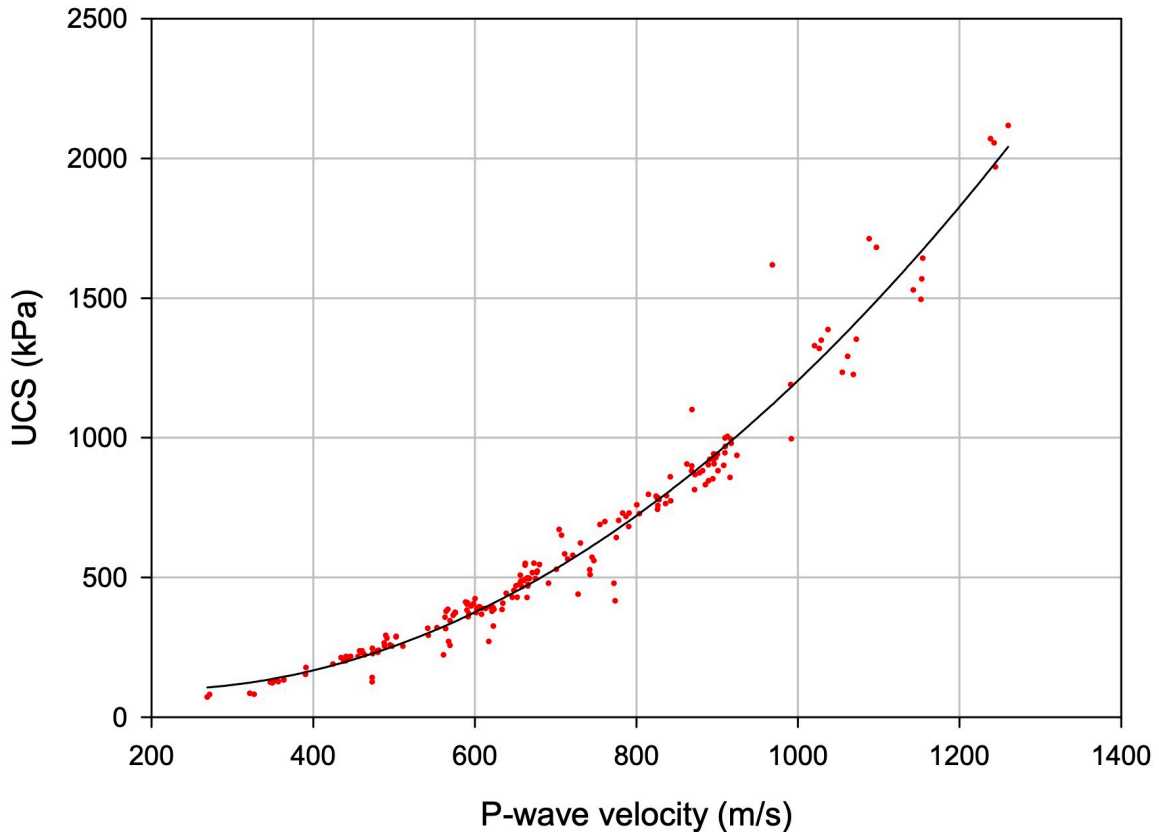


Figure 9. Correlation between P-waves velocity and compressive strength for all samples.

In total, the compressive strength in this study was determined on 194 test specimens. The results shown in Figure 8 demonstrate that at higher values of the compressive strength (increase in Y-axis), the data distribution begin to give a greater spread, which has also been noted in previous studies (Lindh, 2004). The P-wave velocity was determined on all specimens with correlation between the P-wave velocity and compressive strength shown in Figure 9. The correlation between the UCS and binder combinations in specimens was modelled. The regression is reported in Eq. 1 which shows the UCS of the tested specimens as the maximum axial compressive stress that a sample of specimen can withstand under unconfined conditions. Hence the obtained results show the following formula:

$$UCS = 166.172 - 0.668 * P_w + 0.002 * P_w^2 \quad (1)$$

Here the UCS is the unconfined compressive strength of the specimen in kPa, and P_w is the P-wave velocity (m/s). The correlation that model covers 97% of the probability of variation and can be considered as precise.

3.4 Simplex tests on binder content

The slag–cement–CKD simplex diagrams shown changing compressive strength in specimens with different ratio of binder (low/high water and low/high binder content, kg/m³) and various proportions of cement. Even though the slag reached higher values, both cement and CKD exhibited similar effects from adding higher water content. The experiment shows the increased compressive strength at a high slag content in binder mix compared to the pure cement or other mixes. To facilitate the comparison of variation in binder content, the study also evaluated the compressive strength for each combination of cement-CKD-slag in tested specimens, and the corresponding plots are shown in Figures 10, 11 and 12.

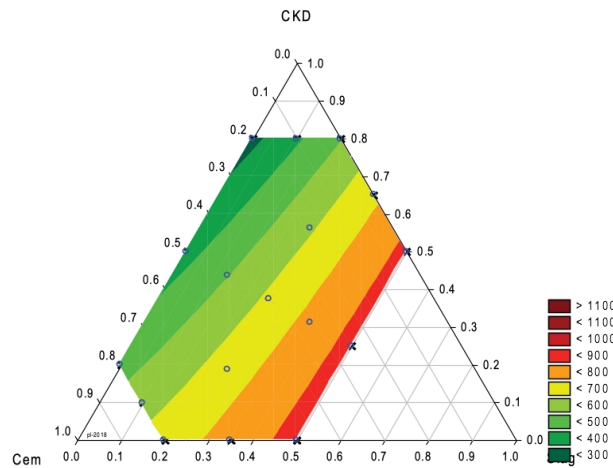


Figure 10. ED1 compressive strength of the specimen by combination of slag, cement and CKD, measured by seismic P-wave velocities.

Figure 10 shows the compressive strength of the specimen by combination of slag, cement and CKD. The values of compressive strength were measured by P-wave velocity by experimental tests starting in ratio of slag=0.5 and CKD=0.5 and pure cement=0.2. The highest compressive strength (>1100 kPa) has been noticed for the following combination (red area in Figure 10): for the specimen with cement=0.5, cement =0.5 to 0.6, CKD=0.5 to 0.53. As the cement increased in the specimen (from 0.3 to 0.45), the initiation of the compressive strength was observed for the interval 700-800 kPa (orange area in Figure 10). The highest values (above 900 kPa) are observed for gradually increasing cement from 0.45 to 0.5 (bright red areas in Figure 10).

Figure 11 displayed various combinations of cement, CKD and slag showing different values of the normalized UCS of specimen in relation to the CO₂ load, of which adding cement from 0.76 shows the highest values of UCS in the samples. In these tests slag was added in combinations from 0 to 0.4; CKD was tested from 0.6 to 0.8 (Figure 11).

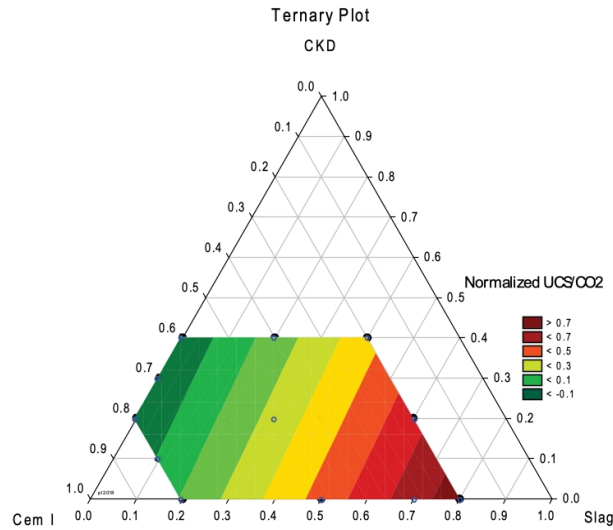


Figure 11. ED2 strength normalized with respect to UCS in relation to CO₂ load.

Significant increases in the compressive strength (values >1500 kPa) were recorded for the highest values of CKD and cement, and relatively low values of slag (Figure 12, bright red colours). In this case, the optimal combination of the slag-cement-CKD was detected at the following values: cement=0.75, slag=0.3, CKD=0.9.

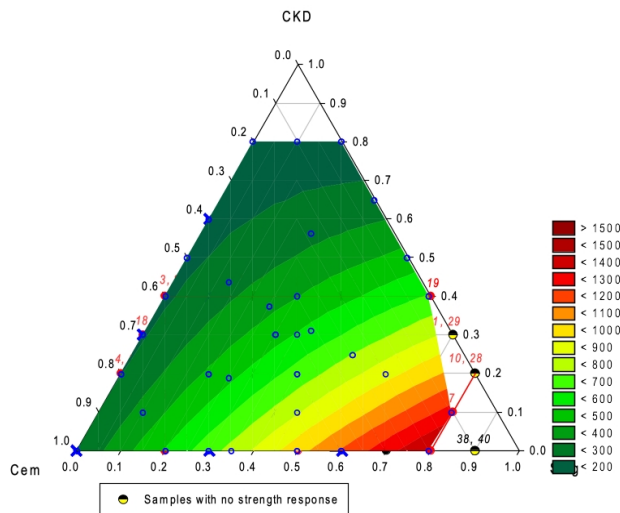


Figure 12. Evaluated compressive strength response surface for ED1 and ED2. Graph, for the factor experiment at 91 days

Figure 12 shows that general increase of the isolines of the compressive strength corresponded to the increase of the amount of cement and decrease of slag, correspondingly. Compared to the cement and slag, the CKD affected the compressive strength in a non-linear way. Ternary

diagrams demonstrated complex relationship between the values of the three variables summing them to a constant, which is represented as 100% [93]. In this study, ternary plots show the correlation between the binder components (cement, slag, CKD) and compressive strength.

4. DISCUSSION AND REFLECTIONS

To evaluate the variations of the compressive strength of the stabilized sediments at different combinations of binder (cement-CKD and slag), we applied seismic testing of samples taken from the port of Gothenburg. The methodology was based on the Swedish Standard practice of testing cement using methods of the resonant frequency of the P-waves, c.f. SS-EN 16907-4. Annex C [94]. We identified the combinations of the cement-slag-CKD that performed best. The goal of this research was to evaluate the compressive strength of specimens by seismic P-wave testing. We statistically visualized the performance of the observed variables by changed two parameters: 1) combinations of binder (cement, CKD and slag); 2) curing time. A total of 194 marine sediment specimens were sampled. The compressive strength correlated with a period of treatment time and the percentage of cement in a mixture.

Seismic methods of P-wave sounding aimed at a better understanding of how the compressive strength changes over time in individual specimens and how it varies by different percentages of cement/slag/water ratios. We found that the P-wave velocity is a function of time for the same sediment with six different water binder numbers. Besides, lower water binder gave higher P-wave velocity, which indicates higher compressive strength. The binder used in this case was 40% cement and 60% slag. Using pure cement as a binder shown different result, which proved the sensitivity of the P-waves to inner structure of the cementitious materials. The paper demonstrated application of the robust geophysical non-destructive methods for evaluation of the compressive strength of the stabilized marine sediments.

Our results further suggest that within a series of tests, the compressive strength was strongly affected by the percentage of cement and CKD, as well as curing time. The presented ternary diagram plots show variations of the compressive strength by different combination of cement, CKD and slag which are mostly affected by the content of cement. The results show that the most suitable binder replacement for cement is the CKD, which is caused by its physical and mechanical properties close to cement. Curing time demonstrated a positive effect on the compressive strength, which is caused by the increasing durability of the stabilized sediments. Seismic testing of the specimens using P-waves shown a correlation between the different combinations of binders (cement/slag/CKD) and curing time. The effects of various water/binder ratio on the performance of sediments were visualized using simplex graphs. The resonant frequency approach shown the impact of varied components of binder on the compressive strength of tested specimens.

5. CONCLUDING REMARKS

Seismic testing of the stabilized marine sediments was conducted to measure compressive strength of the specimens. The study was supported by graphical visualization and comparison of the compressive strength of samples in different binder/water ratio. The correlations between the

UCS, combination of the cement-slag-CKD in various percentage and curing time were modelled and visualized using a series of graphs as ternary diagrams. The study described variations in the reactions of the sediment samples on stress during the P-waves testing. The advantages of seismic and acoustic methods in soil stabilization techniques can be explained by physical and mechanical properties of soils detectable by the P-waves.

The following conclusions can be drawn from the present study:

- The choice of one or another binder proportions for increasing the compressive strength of the soil specimens showed remarkable effects in the results of the evaluation of the strength in the stabilized soil samples. This proved the existing correlation between the percentage of cement in binder used for stabilization of soil and the compressive strength of the soil specimens;
- Besides cement/slag ratio, stress intensity and curing time also play an important role in compressibility of sediments;
- The seismic analysis showed that soil samples with high UCS exhibited higher P-wave velocity in the stabilized sediments. From a geochemical point of view, the porosity might have induced this difference, well reflected in various binder combinations: high water content with low binder = Hw/Lb; high water with high binder = Hw/Hb; low water content with low binder = Lw/Lb; low water content with high binder = Lw/Hb.
- The advantages of the non-destructive remote sensing methods in measurements of the compressive strength enable to examine stabilized sediments with higher resolution and accuracy, lesser destructivity, labour and speed compared to the traditional contact-based methods.

The present method demonstrated advanced seismic methods that can be used in similar works for evaluation of the compressive strength in the stabilized soil specimens [95–99]. Using seismic methods may assist in measuring suitability of soils prior to construction works for evaluating the compressive strength of sampled sediments by resonant frequency [100–101]. The study presented an example of the interdisciplinary approach combining geophysical, geotechnical and statistical approaches. As such, the study is applicable in a variety of domains: construction of roads and highways, tunnels and buildings. Using the remote sensing methods for soil assessment presents a step forward from the traditional methods of evaluating soil properties.

Accurate evaluation of the compressive strength of soil specimens is important for prevention of geotechnical hazards and risks. Constructions on the weak soils may lead to the negative consequences in the infrastructure: cracked asphalt roads and highways, buildings and surfaces. Therefore, evaluating strength of the soil specimens stabilized by various proportions of binder (cement, CKD and slag) can help identify weak soil and avoid construction risks. The study contributed to this task by evaluating the compressive strength of soil specimens stabilized by binders with different percentage of cement, CKD and slag, and various curing time.

DECLARATION OF COMPETING INTEREST

There are no known conflicts of interest associated with this publication. Both authors have read and approved the final manuscript.

ACKNOWLEDGEMENT

The project has been implemented by the support of the Swedish Geotechnical Institute (SGI), GRID-Arendal Project, Gothenburg Harbour, Cementa (HeidelbergCement Group) and help of Annika Åberg. We express our gratitude to the editor Dr. Johan Silfwerbrand and two anonymous reviewers for their reading, comments and suggestions that improved the initial version of the manuscript.

REFERENCES

1. Callister W D Jr & Rethwisch D G: “Materials Science & Engineering an Introduction”. New York: John Wiley & Sons, 2018.
2. Groover M P: “Fundamentals of Modern Manufacturing: Materials, Processes, and Systems”. (7th ed). New York, U.S.A: John Wiley & Sons, 2019.
3. Yin B, Wu C, Hou D, Li S, Jin Z, Wang M & Wang X: “Research and application progress of nano-modified coating in improving the durability of cement-based materials”. *Progress in Organic Coatings*, Vol. 161 (106529), 2021.
4. Research and Markets: “Global Cement Market (2021 to 2026) - Industry Trends, Share, Size, Growth, Opportunity and Forecasts”, 2021.
5. Andersson L, Silfwerbrand J, Selander A & Trägårdh J: “Continuous Preventive Bridge Maintenance of Swedish Municipalities – A Survey on Common Practice”. *Nordic Concrete Research*, No. 58(1), 2018, pp. 127–142.
6. Jalonen K, Tulonen J & Laaksonen A: “Influence of Cracking on Effects of Restrained Deformations in a Post-tensioned Concrete Bridge”. *Nordic Concrete Research*, No. 59(1), 2018, pp. 95–110.
7. Mattsson H-Ä, Sundquist H & Silfwerbrand J: “The Real Service Life and Repair Costs for Bridge Edge Beams / Die reale Nutzungsdauer und Reparaturkosten für Brückenkappen”. *Restoration of Buildings and Monuments*, Vol. 13, no. 4, 2007, pp. 215-228.
8. Vezjanovic J J, Pacoste C & Karoumi R: “Width and Edge Beam Effects on the Ultimate Behaviour of RC Bridge Overhangs”. *Nordic Concrete Research*, No. 61(2), 2019, pp. 131–152.
9. SIS: “Methods of testing cement – Part 1: Determination of strength. Swedish Institute for Standards. Swedish standard SS-EN 196-1:2016”. Swedish Institute for Standards, 2021.
10. Ahmed L: “Dynamic Measurements for Determining Poisson’s Ratio of Young Concrete”. *Nordic Concrete Research*, No. 58(1), 2018, pp. 95–106.
11. Sadagopan M, Malaga K, Lundin M & Nagy A: “Effects of Slag Addition and Mechanical Pre-Processing on the Properties of Recycled Concrete in Terms of Compressive Strength and Workability”. *Nordic Concrete Research*, No. 64(1), 2021, pp. 11–29.
12. Nielsen C V & Kaasgaard M: “Activation Energy for the Concrete Maturity Model – Part 1: Compressive Strength Tests at Different Curing Temperatures”. *Nordic Concrete Research*, No. 62(1), 2020, pp. 87–106.
13. Dahlin T, Svensson M & Lindh P: “DC Resistivity and SASW for Validation of Efficiency in Soil Stabilisation Prior to Road Construction”. In: *Proceedings EEGS’99*, Budapest, Hungary, 6-9 September 1999, pp. 1–3.

14. Mohaghegh A M, Silfwerbrand J & Årskog V: Shear behavior of high-performance basalt fiber concrete—Part II: Laboratory punching shear tests on small slabs with macrofibers without bars. *Structural Concrete*, Vol. 19, 2018, pp. 331–339.
15. Lindh P & Winter M G: “Sample preparation effects on the compaction properties of Swedish fine-grained tills”. *Quarterly Journal of Engineering Geology and Hydrogeology*, Vol. 36, No. 4, 2003, pp. 321–330.
16. Lindh P: “Mcv and shear strength of compacted fine-grained tills”. In: *Proceedings 12th Asian Regional Conference on Soil Mechanics and Geotechnical Engineering*. 4–8 August 2003, Singapore, 2003, pp. 493–496.
17. Lindh P: “Compaction- and strength properties of stabilized and unstabilized fine-grained tills”. ISRN: LUTVDG/TVGT-1013–SE (PhD Thesis). Lund University, Lund, Sweden, 2004, 319 pp.
18. Chang T P, Lin H C, Chang W T & Hsiao J F: “Engineering properties of lightweight aggregate concrete assessed by stress wave propagation methods”. *Cement and Concrete Composites*, Vol. 28, No. 1, 2006, pp. 57-68.
19. Yang Y, Zhou Q, Li X, Lum G C & Deng Y: “Uniaxial compression mechanical property and fracture behavior of hybrid inorganic short mineral fibers reinforced cement-based material”. *Cement and Concrete Composites*, Vol. 104, 2019.
20. Madhusudhan B N, Clayton C R I & Priest J A: (2019). “The effects of hydrate on the strength and stiffness of some sands”. *Journal of Geophysical Research: Solid Earth*, Vol. 124, pp. 65–75.
21. Bharadwaj K, Ghantous R M, Sahan F, Isgor O B & Weiss W J: “Predicting pore volume, compressive strength, pore connectivity, and formation factor in cementitious pastes containing fly ash”. *Cement and Concrete Composites*, Vol. 122, 2021.
22. Wang B & Gupta R: “Analyzing bond-deterioration during freeze-thaw exposure in cement-based repairs using non-destructive methods”. *Cement and Concrete Composites*, Vol. 115, 2021.
23. Lindh P, Ryden N & Ekdah U: “Comparison between unconfined compression test and free-free resonant column test”. In: *Proceedings of 2nd symposium (TREMTE)*, Paris, France, 2005.
24. Rydén N, Ekdahl U & Lindh P: “Quality Control of Cement stabilized Soil using Non-Destructive Seismic Tests”. In: *Conference Proceedings. Advanced Testing of Fresh Cementitious Materials*. August 3-4, 2006, Stuttgart, Germany, 2006, pp. 1-5.
25. Trtnik G & Turk G: “Influence of superplasticizers on the evolution of ultrasonic P-wave velocity through cement pastes at early age”. *Cement and Concrete Research*, Vol. 51, 2013, pp. 22-31.
26. TenCate J A, Malcolm A E, Feng X & Fehler M C: “The effect of crack orientation on the nonlinear interaction of a P wave with an S wave”. *Geophysical Research Letters*, Vol. 43, 2016, pp. 6146–6152.
27. Ryden N, Dahlen U, Lindh P & Jakobsson A: “Impact non-linear reverberation spectroscopy applied to non-destructive testing of building materials”. *The Journal of the Acoustical Society of America*, Vol. 140, No. 4, 2016, pp. 3327-3327.
28. Yan B, Zhu W, Hou C, Yilmaz E & Saadat M: “Characterization of early age behavior of cemented paste backfill through the magnitude and frequency spectrum of ultrasonic P-wave”. *Construction and Building Materials*, Vol. 249, 2020.

29. Halliday D, Resnick R & Walker J: “Fundamentals of Physics”. Part 2. (7th ed.). New York: John Wiley & Sons Ltd, 2005.
30. Červený V: “Seismic Ray Theory”. Cambridge, UK: Cambridge University Press, 2001.
31. Lay T & Wallace T C: “Modern Global Seismology”. San Diego: Academic Press, 1995.
32. Åhnberg H & Holmén M: “Assessment of stabilized soil strength with geophysical methods”. *Ground Improvement*, Vol. 164, No. 3, 2011, pp. 109–116.
33. Verástegui-Flores R D, Di Emidio G, Bezuijen A, Vanwalleghem J & Kersemans M: “Evaluation of the free–free resonant frequency method to determine stiffness moduli of cement-treated soil”. *Soils and Foundations*, Vol. 55, No. 5, 2015, pp. 943-950.
34. Han T, Gurevich B, Pervukhina M, Clennell M B & Zhang J: “Linking the pressure dependency of elastic and electrical properties of porous rocks by a dual porosity model”. *Geophysical Journal International*, Vol. 205, No. 1, 2016, pp. 378–388.
35. Chand S, Minshull T A, Priest J A, Best A I, Clayton C R I & Waite W F: “An effective medium inversion algorithm for gas hydrate quantification and its application to laboratory and borehole measurements of gas hydrate-bearing sediments”. *Geophysical Journal International*, Vol. 166, No. 2, 2006, pp. 543–552.
36. Yoneda J, Jin Y, Katagiri J & Tenma N: “Strengthening mechanism of cemented hydrate-bearing sand at microscales”. *Geophysical Research Letters*, Vol. 43, 2016, pp. 7442–7450.
37. Pan H, Li H, Chen J, Zhang Y, Cai S, Huang Y, Zheng Y, Zhao Y & Deng J: “A unified contact cementation theory for gas hydrate morphology detection and saturation estimation from elastic-wave velocities”. *Marine and Petroleum Geology*, Vol. 113, 2020.
38. Kim H S, Cho G C & Kwon T H: “Effect of CO₂ hydrate formation on seismic wave velocities of fine-grained sediments”. *Geochemistry, Geophysics, Geosystems*, Vol. 14, 2013, pp. 1787–1799.
39. Khaksar A, Griffiths & McCann C: “Compressional- and shear-wave velocities as a function of confining stress in dry sandstones”. *Geophysical Prospecting*, Vol. 47, 1999, pp. 487-508.
40. Yun T S, Francisca F M, Santamarina J C & Ruppel C: “Compressional and shear wave velocities in uncemented sediment containing gas hydrate”. *Geophysical Research Letters*, Vol. 32, No. L10609, 2005.
41. Lindh P, Dahlin T & Svensson M: “Comparisons between different test methods for soil stabilisation”. In: *Proceedings of the ISRM International Symposium 2000*, IS 2000; Melbourne; Australia; 19-24 November 2000, Code 139306, pp. 1–5.
42. Zhu H, Yu H, Ma H & Yang S: “Uniaxial compressive stress-strain curves of magnesium oxysulfate cement concrete”. *Construction and Building Materials*, 232, 2020.
43. Frias Lopez R, Ekblad J & Silfwerbrand J: Resilient properties of binary granular mixtures: A numerical investigation. *Computers and Geotechnics*, Vol. 76, 2016, pp. 222–233.
44. Horii H & Nemat-Nasser S: “Compression-Induced Microcrack Growth in Brittle Solids: Axial Splitting and Shear Failure”. *Journal of Geophysical Research*, Vol. 90, No. B4, 1985, pp. 3105-3125.
45. Hazzard J F & Young R P: “Numerical investigation of induced cracking and seismic velocity changes in brittle rock”. *Geophysical Research Letters*, Vol. 31, 2004.
46. Wang H, Binder E, Mang H, Yuan Y & Pichler B: “Multiscale structural analysis inspired by exceptional load cases concerning the immersed tunnel of the Hong Kong-Zhuhai-Macao Bridge”. *Underground Space*, Vol. 3, No. 4, 2018, pp. 252-267.
47. Zhang W, Han L, Gu X, Wang L, Chen F & Liu H: “Tunneling and deep excavations in spatially variable soil and rock masses: A short review”. *Underground Space*, 2020.

48. Larsen I L, Terjesen O, Thorstensen R T & Kanstad T: “Use of Concrete for Road Infrastructure: A SWOT Analysis Related to the three Catchwords Sustainability, Industrialisation and Digitalisation”. *Nordic Concrete Research*, No. 60(1), 2019, pp. 31–50.
49. Chung C W, Suraneni P, Popovics J S & Struble L J: “Using ultrasonic wave reflection to monitor false set of cement paste”. *Cement and Concrete Composites*, Vol. 84, 2017, pp. 10–18.
50. Palomar I & Barluenga G: “Assessment of lime-cement mortar microstructure and properties by P- and S- ultrasonic waves”. *Construction and Building Materials*, Vol. 139, 2017, pp. 334-341.
51. Lootens D, Schumacher M, Liard M, Jones S Z, Bentz D P, Ricci S & Meacci V: “Continuous strength measurements of cement pastes and concretes by the ultrasonic wave reflection method”. *Construction and Building Materials*, Vol. 242, 2020.
52. Miró M, Eiras J N, Poveda P, Climent M A & Ramis J: “Detecting cracks due to steel corrosion in reinforced cement mortar using intermodulation generation of ultrasonic waves”. *Construction and Building Materials*, Vol. 286, 2021.
53. Han Z, Li D, Zhou T, Zhu Q & Ranjith P G: “Experimental study of stress wave propagation and energy characteristics across rock specimens containing cemented mortar joint with various thicknesses”. *International Journal of Rock Mechanics and Mining Sciences*, Vol. 131, 2020.
54. Lagarde J, Abraham O, Laguerre L, Côte P, Piguet J P, Balland C & Armand G: “Use of surface waves and seismic refraction for the inspection of circular concrete structures”. *Cement and Concrete Composites*, Vol. 28, No. 4, 2006, pp. 337-348.
55. Niederleithinger E & Taffe A: “Early stage elastic wave velocity of concrete piles”. *Cement and Concrete Composites*, Vol. 28, No. 4, 2006, pp. 317-320.
56. Trtnik G & Gams M: (2013). “The use of frequency spectrum of ultrasonic P-waves to monitor the setting process of cement pastes”. *Cement and Concrete Research*, Vol. 43, pp. 1-11.
57. Sleep N H & Erickson B A: “Nonlinear attenuation of S-waves and Love waves within ambient rock”. *Geochemistry, Geophysics, Geosystems*, Vol. 15, 2014, pp. 1419–1440.
58. Zhan L & Matsushima J: “Frequency-dependent P-wave attenuation in hydrate-bearing sediments: a rock physics study at Nankai Trough, Japan”. *Geophysical Journal International*, Vol. 214, No. 3, 2018, pp. 1961–1985.
59. Källén H, Heyden A & Lindh P: “Estimation of grain size in asphalt samples using digital image analysis”. In: *Proceedings of SPIE – The International Society for Optical Engineering*, 2014.
60. Källén H, Heyden A, Åström K & Lindh P: Measuring and evaluating bitumen coverage of stones using two different digital image analysis methods. *Measurement*, Vol. 84, 2016, pp. 56–67.
61. Lemenkov V & Lemenkova P: “Using TeX Markup Language for 3D and 2D Geological Plotting”. *Foundations of Computing and Decision Sciences*, Vol. 46, 2021, pp. 43–69.
62. Lemenkov V, Lemenkova P: “Measuring Equivalent Cohesion C_{eq} of the Frozen Soils by Compression Strength Using Kriolab Equipment”. *Civil and Environmental Engineering Reports*, Vol. 31, No. 2, 2021, pp. 63–84.
63. Xuequan W, Sheng Y, Xiaodong S, Mingshu T & Liji Y: “Alkali-activated slag cement based radioactive waste forms”. *Cement and Concrete Research*, Vol. 21, No. 1, 1991, pp. 16-20.

64. Zhu D, Mobasher B & Rajan S D: “Non-contacting strain measurement for cement-based composites in dynamic tensile testing”. *Cement and Concrete Composites*, Vol. 34, No. 2, 2012, pp. 147-155.
65. Oucif C & Mauludin L M: “Numerical modeling of high velocity impact applied to reinforced concrete panel”. *Underground Space*, Vol. 4, No. 1, 2019, pp. 1-9.
66. Uppalapati S, Vandewalle L & Cizer Ö: “Monitoring the setting process of alkali-activated slag-fly ash cements with ultrasonic P-wave velocity”. *Construction and Building Materials*, Vol. 271, 2021.
67. Meng T, Hong Y, Ying K & Wang Z: “Comparison of technical properties of cement pastes with different activated recycled powder from construction and demolition waste”. *Cement and Concrete Composites*, Vol. 120, 2021.
68. Lahdensivu J, Kekäläinen P & Lahdensivu A: “Alkali-silica Reaction in Finnish Concrete Structures”. *Nordic Concrete Research*, No. 59(1), 2018, pp. 31–44.
69. Ogata T & Osada K: “Seismic retrofitting of expressway bridges in Japan”. *Cement and Concrete Composites*, 22(1), 2000, pp. 17–27.
70. Matsumoto N, Kitago Y & Sato T: “Restoration, seismic strengthening and seismic design for railway viaducts after Hyogoken-Nanbu Earthquake”. *Cement and Concrete Composites*, Vol. 22, No. 1, 2000, pp. 47–57.
71. Fabozzi S, Licata V, Autuori S, Bilotta E, Russo G & Silvestri F: “Prediction of the seismic behavior of an underground railway station and a tunnel in Napoli (Italy)”. *Underground Space*, Vol. 2, No. 2, 2017, pp. 88–105.
72. Arora K, Gutierrez M, Hedayat A & Xia C: “Tunnels in squeezing clay-rich rocks”. *Underground Space*, 2020.
73. Lindh P: “Optimizing binder blends for shallow stabilisation of fine-grained soils”. *Ground Improvement*, Vol. 5, 2001, pp. 23–34.
74. Singh J, Cilli P A, Hosa, A & Main I G: “Digital rock physics in four dimensions: simulating cementation and its effect on seismic velocity”. *Geophysical Journal International*, Vol. 222, No. 3, 2020, pp. 1606–1619.
75. Revert A B, De Weerd K, Jakobsen U H & Geiker M R: “Impact of Accelerated Carbonation on Microstructure and Phase Assemblage”. *Nordic Concrete Research*, No. 59(1), 2018, pp. 111–126.
76. Li G & Zhao X: “Properties of concrete incorporating fly ash and ground granulated blast-furnace slag”. *Cement and Concrete Composites*, Vol. 25, No. 3, 2003, pp. 293–299.
77. Badrawi E F & El-kady M S: “Stabilizing soft clay using geo-foam beads and cement bypass dust”. *Underground Space*, Vol. 5, No. 4, 2020, pp. 292-297.
78. Mavko G, Mukerju T & Dvorkin J: “The Rock Physics Handbook”. Cambridge, UK: Cambridge University Press, 1998.
79. Khan Z, Majid A, Cascante G, Hutchinson D J & Pezeshkpour P: “Characterisation of a cemented sand with the pulse-velocity method”. *Canadian Geotechnical Journal*, Vol. 43, 2006, pp. 294–309.
80. Eisner L, Fischer T & Rutledge J T: “Determination of S-wave slowness from a linear array of borehole receivers”. *Geophysical Journal International*, Vol. 176, No. 1, 2009, pp. 31–39.
81. Xu N, Song Z, Guo M Z, Jiang L, Chu H, Pei C, Yu P, Liu Q & Li Z: “Employing ultrasonic wave as a novel trigger of microcapsule self-healing cementitious materials”. *Cement and Concrete Composites*, Vol. 118, 2021.

82. SIS: “Standard Test Methods for Downhole Seismic Testing”. ASTM standard. ASTM D7400/D7400M-19. Swedish Institute for Standards, 2021.
83. SIS: “Standard Guide for Using the Seismic Refraction Method for Subsurface Investigation”. ASTM standard. ASTM D5777-18. Swedish Institute for Standards, 2021.
84. Lillie R J: “Whole Earth Geophysics. An Introductory Textbook for Geologists and Geophysicists”. Oregon State University. U.S.A: Prentice Hall, 1999.
85. Sheriff R E, Geldart L P: “Exploration Seismology”. (2nd ed.). Cambridge, UK: Cambridge University Press, 1995.
86. Schlumberger Oilfield Glossary: “P-wave”, 2021.
87. Schlumberger Oilfield Glossary: “S-wave”, 2021.
88. SIS: “Geotechnical investigation and testing – Laboratory testing of soil – Part 7: Unconfined compression test (ISO 17892-7:2017)”. Swedish Institute for Standards, 2021.
89. Myers R H, Montgomery D C & Anderson-Cook C M: “Response Surface Methodology: Process and Product Optimization Using Designed Experiments”. 4th Ed. New York, U.S.A: John Wiley & Sons, 2016.
90. Jersak J, Göransson G, Ohlsson Y, Larsson L, Flyhammar P & Lindh P: “In-situ övertäckning av förorenade sediment. Metodöversikt”. SGI Publikation 30-1, Statens geotekniska institut, Linköping, 2016.
91. Smith W F: “Experimental design for formulation”. ASA-SIAM Series on Statistics and Applied Probability, SIAM, Philadelphia, ASA, Alexandria, VA, 2005.
92. Montgomery D C: *Design and Analysis of Experiment*. New York: John Wiley & Sons, 1996.
93. Lemenkova P: “Statistical Analysis of the Mariana Trench Geomorphology Using R Programming Language”. *Geodesy and Cartography*, Vol. 45, No. 2, 2019, pp. 57–84.
94. SIS: “Earthworks – Part 4: Soil treatment with lime and/or hydraulic binders”. 2018-12-12, 2018.
95. Aki K & Richards P G: “Quantitative Seismology, Vol. 1: Theory and Methods”. W H Freeman & Co, 1980.
96. Bullen K E & Bolt B A: “An Introduction to the Theory of Seismology”. 4th ed. Cambridge: Cambridge University Press, 1985.
97. Dahlen F A & Tromp J: “Theoretical Global Seismology”. New Jersey: Princeton University Press, 1999.
98. Newman W I: “Mathematical Methods for Geophysics and Space Physics Mathematical Methods for Geophysics and Space Physics”. New Jersey: Princeton University Press, 2016.
99. Wang Y, Yuan Q, Deng D & Liu Z: “Modeling compressive strength of cement asphalt composite based on pore size distribution”. *Construction and Building Materials*, Vol. 150, 2017, pp. 714–722.
100. Su J, Wang J, Li Z, Liang X: “Effect of reinforcement grade and concrete strength on seismic performance of reinforced concrete bridge piers”. *Engineering Structures*, Vol. 198, 2019.
101. Zhang X, Yang Z, Chen X, Guan J, Pei W & Luo T: “Experimental study of frozen soil effect on seismic behavior of bridge pile foundations in cold regions”. *Structures*, Vol. 32, 2021, pp. 1752–1762.

APPENDIX A

Nonlinear Regression report from the Sigmaplot 14:

Data Source: Data 2 in VBT

Equation: Hyperbola, Single Rectangular, 2
Parameter

$$f = a*x/(b+x)$$

R Rsqr Adj Rsqr Standard Error of Estimate

0.996 0.992 0.983 9.883

Coefficient Std. Error t P

a 697.546 13.068 53.379 0.0119

b 5.286 0.589 8.973 0.0707

Analysis of Variance:

DF SS MS

Regression 2 1035288.445 517644.222

Residual 1 97.680 97.680

Total 3 1035386.125 345128.708

Corrected for the mean of the observations:

DF SS MS

Regression 1 11536.361 11536.361

Residual 1 97.680 97.680

Total 2 11634.042 5817.021

Statistical Tests:

Normality Test (Shapiro-Wilk) Passed (P = 0.0890)

W Statistic= 0.7892 Significance Level = 0.0500

Constant Variance Test (Spearman Rank Correlation) Failed (P = <0.0001)

Fit Equation Description:

[Variables]

x = col(1)

y = col(2)

reciprocal_y = 1/abs(y)

reciprocal_ysquare = 1/y^2

reciprocal_x = 1/abs(x)

reciprocal_xsquare = 1/x^2

reciprocal_pred = 1/abs(f)

reciprocal_predsqr = 1/f^2

weight_Cauchy = 1/(1+4*(y-f)^2)

[Parameters]

a = max(y) "Auto {{previous: 697.546}}

b = if(x50(x,y,0.1)<>0, x50(x,y,0.1), 1)

"Auto {{previous: 5.28645}}

[Equation]

f = a*x/(b+x)

fit f to y

"fit f to y with weight reciprocal_y

"fit f to y with weight reciprocal_ysquare

"fit f to y with weight reciprocal_x

"fit f to y with weight reciprocal_xsquare

"fit f to y with weight reciprocal_pred

"fit f to y with weight reciprocal_predsqr

"fit f to y with weight weight_Cauchy

[Constraints]

[Options]

tolerance=1e-10

stepsize=1

iterations=200

Number of Iterations Performed = 8